

**Characterizing many-body localization via state sensitivity to boundary conditions**Mohammad Pouranvari <sup>\*</sup>*Department of Physics, Faculty of Basic Sciences, University of Mazandaran, P. O. Box 47416-95447, Babolsar, Iran*Shiuan-Fan Liou <sup>†</sup>*private sector*

(Received 21 July 2020; revised 6 October 2020; accepted 18 November 2020; published 22 January 2021)

We introduce characterizations for many-body phase transitions between delocalized and localized phases based on the system's sensitivity to boundary conditions. In particular, we change boundary conditions from periodic to antiperiodic and calculate a shift in the system's energy and shifts in the single-particle density-matrix eigenvalues in the corresponding energy window. We employ the typical model for studying MBL, a one-dimensional disordered system of fermions with nearest-neighbor repulsive interaction where disorder is introduced as randomness on on-site energies. By calculating numerically the shifts in the system's energy and eigenvalues of the single-particle density matrix, we observe that in the localized regime, both shifts are vanishing; while in the extended regime, both shifts are on the order of the corresponding level spacing. We also applied these characterizations of the phase transition to the case of having next-nearest-neighbor interactions in addition to the nearest-neighbor interactions and studied its effect on the transition.

DOI: [10.1103/PhysRevB.103.035136](https://doi.org/10.1103/PhysRevB.103.035136)**I. INTRODUCTION**

In a free fermion model with extending plane-wave eigenfunctions, fermions move freely in the entire system. Introducing randomness in the free fermion model, which represents disorder, leads to the localization of fermions due to the quantum interference, proposed by Anderson [1]. This phenomenon, so-called Anderson localization, has been widely studied numerically, analytically, and experimentally. In general, the Anderson localization is associated with the symmetry and dimension of the system [2]. For one- and two-dimensional systems, any infinitesimal uncorrelated randomness makes the system localized [3]. For a three-dimensional (3D) system, however, there exists a nonzero critical disorder strength at which a quantum phase transition between the localized and delocalized phase occurs [4]. In a weak randomness regime, the system is delocalized; as the disorder strength increases and hits the critical value, the system becomes localized. Additionally, a phase transition from a delocalized to a localized phase can be seen in the energy resolution if the system under study has mobility edges. A 3D Anderson model, for example, has localized phases at both tails of the energy spectrum and delocalized phases in the middle of the spectrum [5,6]. Thus as the system's energy changes from one energy window to another, it will undergo a phase transition between localized and delocalized phases.

Another interesting phenomenon arises when interaction is introduced in the Anderson model, from whence we encounter the following questions: Does disorder suppress the effect of the interaction? Or Is the interaction effect so strong that it

makes the interacting system delocalized? More interestingly, what role does temperature play in such a system? We can also ask these questions from the perspective of statistical physics: It is assumed that a classical ergodic system can visit its whole phase space after a finite time, so the averaging of a physical quantity over time is the same as averaging over the whole phase space. In this perspective, the question of the ergodicity of a random interacting system is important [7]. Answering the above questions is currently a hot research topic. By now, we know that in the interacting systems, at a nonzero temperature a phase transition between localized and delocalized phases arises by varying disorder strength [8,9]. In the strong disorder regime, the conductivity—even at a nonzero temperature—is zero, and the state of the system is localized in Fock space. The phase is thus called a many-body localized (MBL) phase [10–13]. The states in the MBL phase do not thermalize in the sense that after a long time, its properties still depend on the initial state of the system (i.e., local integrals of motion constrain the system); in other words, the system carries the information of the initial states [7]. Thus an MBL phase is an out-of-equilibrium phase, and the laws of statistical mechanics are not obeyed. On the other hand, in the weak disorder regime a part of the system acts as a bath for the remainder, such that the eigenstate thermalization hypothesis (ETH) [14–17] can be applied and the system thermalizes. In addition, an ETH-MBL phase transition can be seen at a fixed disorder strength in the energy resolution, i.e., the mobility edges can also be seen in the interacting system [18,19]. Experimentally, the phase transition between the ETH and MBL phases has been witnessed in many systems, such as ultracold atoms [20], trapped ion systems [21], optical lattices [22–28], and quantum information devices [29].

In the remainder of this section, we first cite models with ETH-MBL phase transitions. Then we mention some of the

<sup>\*</sup>m.pouranvari@umz.ac.ir<sup>†</sup>coarliu6@gmail.com

previously studied ETH-MBL phase transition characterizations along with our characterization. The typical model employed to study the ETH-MBL phase transition is the spinless fermion model with constant nearest-neighbor (NN) hopping and NN interactions (which is the Jordan-Wigner transformation of the XXZ model for the spin 1/2); disorder is introduced by random on-site energies. Some studies have also introduced random interactions into the system [30–32]. Having an MBL phase in translation-invariant Hamiltonians and systems with a delocalized single-particle spectrum have also been investigated [32–35]. Although disorder is usually described by random on-site energies, some studies reported that on-site energies with incommensurate periodicity could trigger ETH-MBL phase transitions [19,36,37]; other systems, such as a frustrated spin chain [38] and a system under strong electric field [39], also exhibit ETH-MBL phase transitions.

Finding a characterization for the ETH-MBL phase transition is part of the current research. Entanglement entropy (EE) is one candidate that shows distinguished behavior in the ETH and MBL phases [40,41]. To calculate EE, one divides the system into two subsystems  $A$  and  $B$ ; the reduced density matrix of each subsystem  $\rho_{A/B}$  is calculated by tracing over degrees of freedom of other subsystems. EE then can be calculated as  $EE = -\text{tr} \rho_{A/B} \log \rho_{A/B}$  [2,42]. EE follows an area-law behavior in the MBL phase [43,44], while it obeys volume law in the ETH phase, where the reduced density matrix of a subsystem approaches the thermal density matrix. EE thus fluctuates strongly around the localization-delocalization transition point [45]. In addition, the statistics of the low-energy entanglement spectrum (eigenvalues of the reduced density matrix) have been used as a characterization of the phase transition. The entanglement spectrum distribution goes from Gaussian orthogonal in the extended regime to a Poisson distribution in the localized regime [46]. Furthermore, people have used the eigenenergies level spacing [47] and level dynamics [48] as characterizations. Some other methods, such as machine learning, are also used for detecting the MBL phase transition [49]. These are just a few, among many others [19,37,46,50,51].

A recent paper [52] studied the single-particle density matrix to distinguish MBnL from the ETH phase. The single-particle density matrices are constructed by the eigenstates of the Hamiltonian ( $H$ ) of the system in a target energy window through

$$\rho_{ij} = \langle \psi | c_i^\dagger c_j | \psi \rangle, \quad (1)$$

where  $i$  and  $j$  go from 1 to  $L$  (system size), and  $|\psi\rangle$  is the eigenstate of the Hamiltonian. They studied eigenvalues  $\{n\}$  and eigenfunctions of the density matrix,  $|\phi_k\rangle$ . Its eigenvalues, which can be interpreted as occupations of the orbitals, demonstrate the Fock-space localization: Deep in the delocalized phase,  $\{n\}$ 's are evenly spaced between 0 and 1, while in the localized phase, they tend to be very close to either 0 or 1. Thus the difference between two successive eigenvalues of  $\rho$  shows different behavior in the delocalized and localized phases. Moreover, they found that eigenfunctions of the density matrix  $|\phi_k\rangle$  are extended (localized) in delocalized (localized) phase [53,54].

We, in this paper, look at the ETH-MBL phase transition from the perspective of boundary-condition effects on

the system, namely, we change the boundary conditions from periodic to antiperiodic and then study their effects on the system's energy as well as on the eigenvalues of the single-particle density matrix ( $\rho$ ) at a given energy window (see Sec. II for more details). Our work is a generalization of Ref. [55], where Anderson localization in free fermion models is characterized based on the response of the system to the change in the boundary conditions. The response of an interacting system to a local perturbation, on the other hand, is also investigated in Refs. [56] and [57] as a characterization of the MBL phase, which is analogous to our work.

Results of our work, in brief, are as follows. In contrast to the MBL phase, the system's energy and occupation numbers are sensitive to the boundary conditions in the ETH phase. In MBL phase, shifts in the system's energy and occupation numbers are vanishing; however, in ETH phase, both shifts are on the order of the corresponding level spacing. We use these metrics in a previously studied model with NN interactions that has a known ETH-MBL phase transition. We also apply these characterizations to a model having both NN and NNN interactions.

The paper's structure is as follows. We first introduce the model and explain the numerical method in Sec. II. The responses of the Hamiltonian's eigenenergy and the single-particle density-matrix eigenvalues to the boundary conditions, considering only the NN interaction, are presented in Secs. III and IV, respectively. In Sec. V, we introduce the NNN interaction in the model and consider its effect. We close with some remarks in Sec. VI.

## II. METHOD AND MODEL

We consider spinless fermions confined on a one-dimensional (1D) chain with the nearest-neighbor (NN) hopping; NN and next-nearest-neighbor (NNN) repulsive density-density interactions, as well as diagonal disorder. The effective Hamiltonian can be written as

$$\begin{aligned} H = & -t \sum_{i=1}^L (c_i^\dagger c_{i+1} + \text{H.c.}) + \sum_{i=1}^L \mu_i \left( n_i - \frac{1}{2} \right) \\ & + V_1 \sum_{i=1}^L \left( n_i - \frac{1}{2} \right) \left( n_{i+1} - \frac{1}{2} \right) \\ & + V_2 \sum_{i=1}^L \left( n_i - \frac{1}{2} \right) \left( n_{i+2} - \frac{1}{2} \right), \end{aligned} \quad (2)$$

where  $c_i^\dagger (c_i)$  is the fermionic creation (annihilation) operator, creating (annihilating) a fermion on the site  $i$ , and  $n_i = c_i^\dagger c_i$  is the number operator. The first term in the Hamiltonian is the NN hopping with constant strength  $t$ , which is used as the energy unit in our calculations and is set to unity. The randomized on-site energies, as a disorder representation, are described by  $\mu$ 's. They follow uniform distribution within  $[-W, W]$ , where  $W$  is called disorder strength. The last two terms in the Hamiltonian are the constant repulsive NN and NNN density-density interactions.

To apply boundary conditions, we set  $c_{i+L}^{(\dagger)} = c_i^{(\dagger)}$  for the periodic boundary condition (PBC) and  $c_{i+L}^{(\dagger)} = -c_i^{(\dagger)}$  for the antiperiodic boundary condition (APBC), where  $L$  is

the length of the 1D chain. We first diagonalize the Hamiltonian through the exact diagonalization method and find its eigenvectors and the corresponding eigenvalues. We use the parameter  $\epsilon$ , which is defined as  $\epsilon = \frac{(E-E_0)}{(E_{\max}-E_0)}$ , where  $E$  is the target energy,  $E_0$  is the ground-state energy, and  $E_{\max}$  represents the highest energy in the spectrum; it changes between 0 and 1, corresponding to the ground state and highest energy, respectively. We focus on a certain energy window of the spectrum: For a given  $\epsilon$ , we calculate the target energy  $E$  and select six eigenstates of  $H$  with the energy closest to  $E$ . For each of these six eigenstates, we build up the single-particle density matrix  $\rho$  from Eq. (1). By changing the boundary conditions from PBC to APBC, we calculate the energy shift for each eigenstate:

$$\delta E_i = |E_{i,PBC} - E_{i,APBC}|, \quad (3)$$

where  $E_i$  is the energy of the  $i$ th eigenstate; in this way, the  $i$ th level of the Hamiltonian with PBC is compared with the  $i$ th level of the Hamiltonian with APBC. We then take typical averaging over six eigenstates and take a typical disorder average to obtain  $\delta E^{typ}$  (typical average of the random variable  $x$  is  $e^{\langle \ln x \rangle}$ , where  $\langle \dots \rangle$  stands for arithmetic mean). In the same manner, we calculate shifts in the eigenvalues of the single-particle density matrix:

$$\delta n_i^{(j)} = |n_{i,PBC}^{(j)} - n_{i,APBC}^{(j)}|. \quad (4)$$

A typical average on all eigenvalues of the  $\rho$  ( $j$  goes from 1 to  $L$ ), another typical average over the six samples, and a typical disorder average will be calculated to obtain  $\delta n^{typ}$ .

### III. EFFECT OF THE BOUNDARY CHANGE ON THE ENERGY

In a free fermion model, the state of the system is the Slater determinant of the occupied single-particle eigenstates. In the localized phase, occupied eigenstates of the system are confined in a small region of space, while in the delocalized phase, they spread over the entire system. In Ref. [55], the effect of the change in the boundary conditions on the single-particle eigenenergies of a free fermion model is studied. By changing the boundary conditions in the localized phase, the single-particle energy does not change. On the other hand, in the delocalized phase, where eigenstates of the system are extended, any changes in the boundary conditions can be seen by the wave function; these changes are then reflected in the corresponding energy. Accordingly, the energy shift for each level,  $\delta E$ , divided by the average level spacing  $\Delta E$ , known as Thouless conductance, is a characterization of the Anderson phase transition between delocalized and localized phases:

$$g_E = \delta E / \Delta E. \quad (5)$$

We conjecture that if we change boundary conditions for an interacting system, a similar quantity such as Thouless conductance (now for the system's energy rather than the single-particle eigenenergy), can be used to characterize the phase transition. In particular, we change the condition from periodic to antiperiodic (as explained in Sec. II) and calculate  $g_E$  for the system's energy. In Fig. 1 typical averaged  $g_E$  is plotted for some selected values of the energy for the case of NN interaction of Eq. (2), corresponding to  $V_1 = 1, V_2 = 0$  (standard deviation of  $g_E$  is plotted in Fig. 7). We see that deep

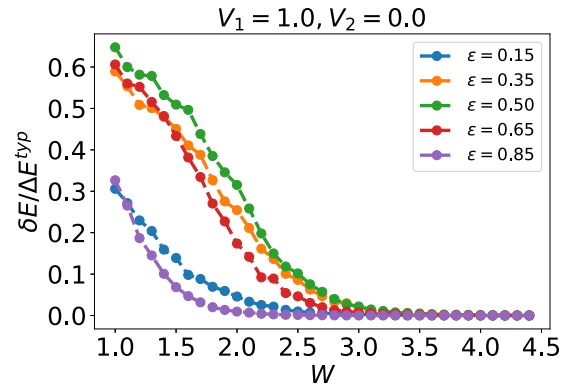


FIG. 1. Typical averaged  $g_E = \frac{\delta E}{\Delta E}$  for the case of having only NN interaction ( $V_1 = 1, V_2 = 0$ ) for some selected  $\epsilon$  as disorder strength  $W$  varies. We set  $L = 14, N = 7$ . We take a typical disorder average over altogether 2000 samples for each data point.

in the delocalized phase, the shift in the system's energy is on the order of level spacing, while deep in the localized phase, the shift is negligible compare to the delocalized phase. Based on this plot, in the middle of the spectrum ( $\epsilon = 0.5$ ),  $g_E$  goes to zero at  $W \approx 3.5$ , consistent with the previously obtained results [56,58–60]. Also,  $g_E$  is plotted for the whole spectrum of energy in Fig. 2 as we vary the disorder strength  $W$ . This plot is also consistent with the previously obtained results.

### IV. EFFECT OF THE BOUNDARY CHANGE ON THE SINGLE-PARTICLE DENSITY MATRIX

We now focus on the effect of boundary conditions on the occupation numbers of density matrix Eq. (1). First, let us look at the case of free fermions, where we can write the Hamiltonian of the system as

$$H_{\text{Free fermion}} = \sum_{i,j=1}^L h_{ij} c_i^\dagger c_j. \quad (6)$$

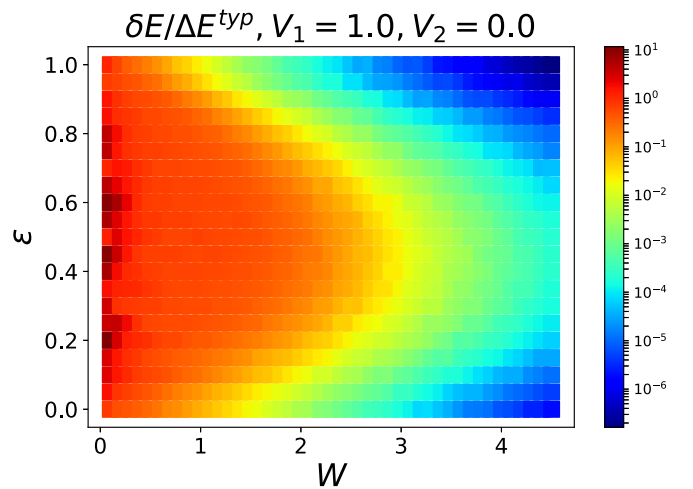


FIG. 2. Typical average of  $g_E = \frac{\delta E}{\Delta E}$  for the entire spectrum of the energy as we change the disorder strength  $W$  for the NN interaction case ( $V_1 = 1, V_2 = 0$ ). System size  $L = 14, N = 7$ . We take typical disorder average over altogether 2000 samples for each data point.

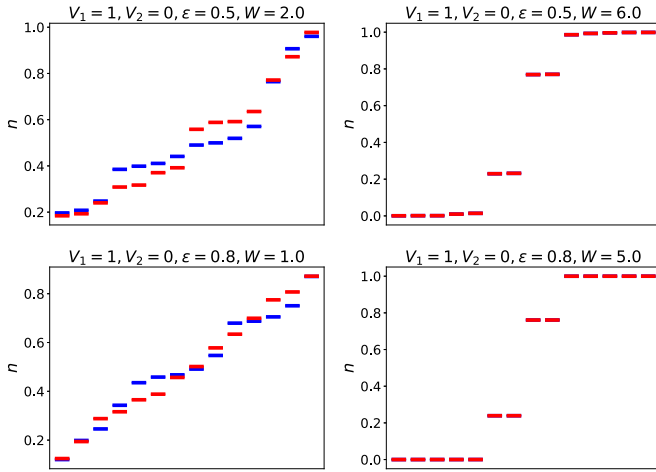


FIG. 3. Eigenvalues of the single-particle density matrix (occupation numbers  $\{n\}$ ) corresponding to periodic boundary condition (blue) and antiperiodic boundary condition (red) for NN interaction of Eq. (2) ( $V_1 = 1, V_2 = 0$ ). In left plots,  $\epsilon$  and  $W$  are chosen such that we are in the extended phase, while in the right plots they correspond to the MBL phase. We set  $L = 14, N = 7$ . Only one sample is considered, and we do not take a disorder average. We see that shifts in the occupation numbers in the MBL phase are almost zero, while the shifts are appreciable in the extended phase.

We observe that eigenfunctions of the single-particle density matrix and matrix  $h$  are the same (both can be diagonalized by the same unitary matrix):

$$h_{ij} = \sum_k U_{ik} \epsilon_k U_{kj}^\dagger, \quad (7)$$

$$\rho_{ij} = \sum_k U_{ik} n_k U_{kj}^\dagger, \quad (8)$$

where  $\epsilon_k$  is the single-particle eigenenergy of the Hamiltonian. By the argument of Thouless [55] that single-particle eigenstates of the Hamiltonian are sensitive (insensitive) to the boundary conditions in the delocalized (localized) phase,

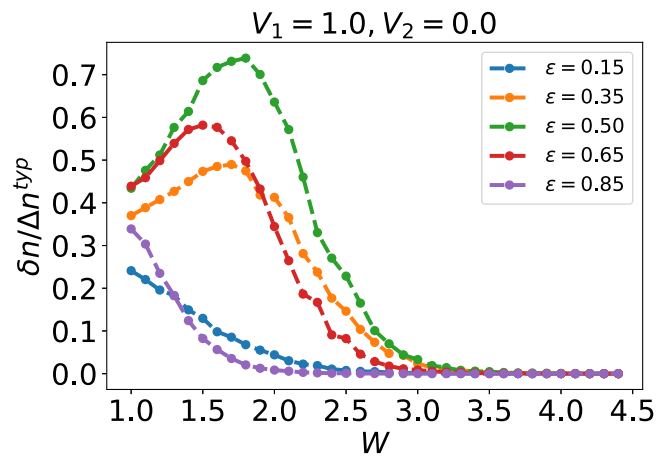


FIG. 4. Typical averaged  $g_n = \frac{\delta n}{\Delta n}$  for the NN interaction case of Eq. (2) corresponding to  $V_1 = 1, V_2 = 0$  for some selected values of  $\epsilon$ 's as we change the disorder strength  $W$ . We set  $L = 14, N = 7$ . We take the typical average over altogether 2000 samples for each data point.

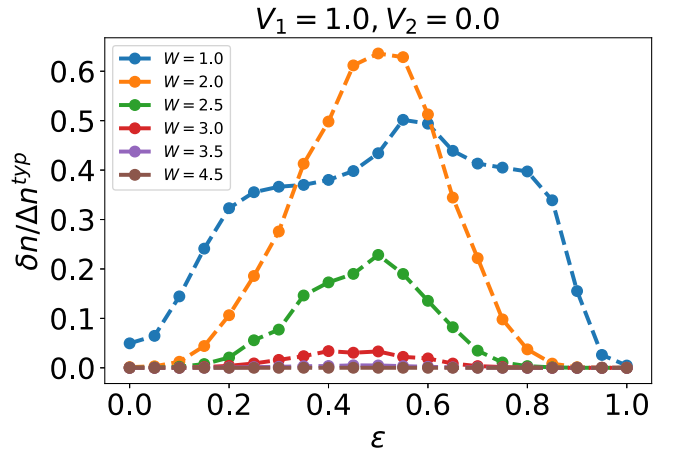


FIG. 5. Typical averaged  $g_n = \frac{\delta n}{\Delta n}$  for the NN interaction case of Eq. (2) corresponding to  $V_1 = 1, V_2 = 0$  for some selected values of disorder strength  $W$  as energy varies, where we can see the mobility edges. We set  $L = 14, N = 7$ . We take the typical average over altogether 2000 samples for each data point.

we can say that eigenvalues of  $\rho$  are sensitive (insensitive) to the boundary conditions in the delocalized (localized) phase. Thus we can identify the shifts in the eigenvalues of  $\rho$  when we change the boundary condition from periodic to antiperiodic as a probe of the phase transition.

This idea has been verified indirectly before: We know that for a free fermion system divided into two subsystems, the reduced density matrix of each subsystem can be written as  $\exp(-H_{\text{ent}})$ , where  $H_{\text{ent}}$  is called entanglement Hamiltonian and can be obtained from the single-particle density matrix of the corresponding subsystem [61]. The effect of the boundary-condition changes on the entanglement Hamiltonian for free fermion models was studied in Ref. [62]. A boundary condition is changed from periodic to antiperiodic, and shifts in the eigenvalues of the entanglement Hamiltonian (and thus on

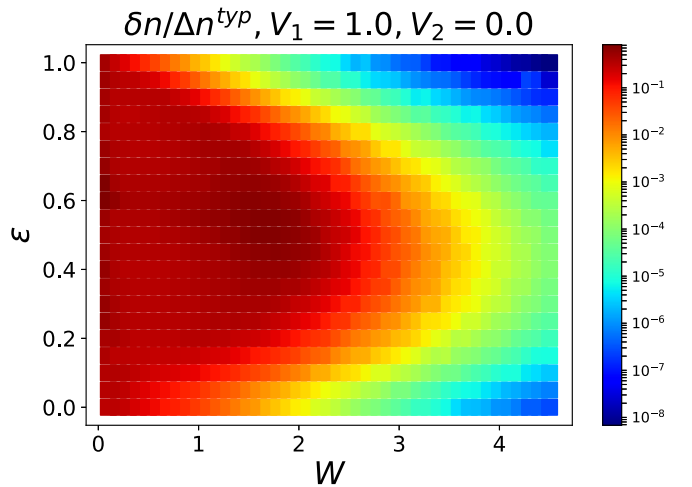


FIG. 6. Typical averaged  $g_n = \frac{\delta n}{\Delta n}$  for the NN interaction case of Eq. (2) corresponding to  $V_1 = 1, V_2 = 0$  for the entire energy spectrum as we change the disorder strength  $W$ . We set  $L = 14, N = 7$ . We take the typical average over altogether 2000 samples for each data point.

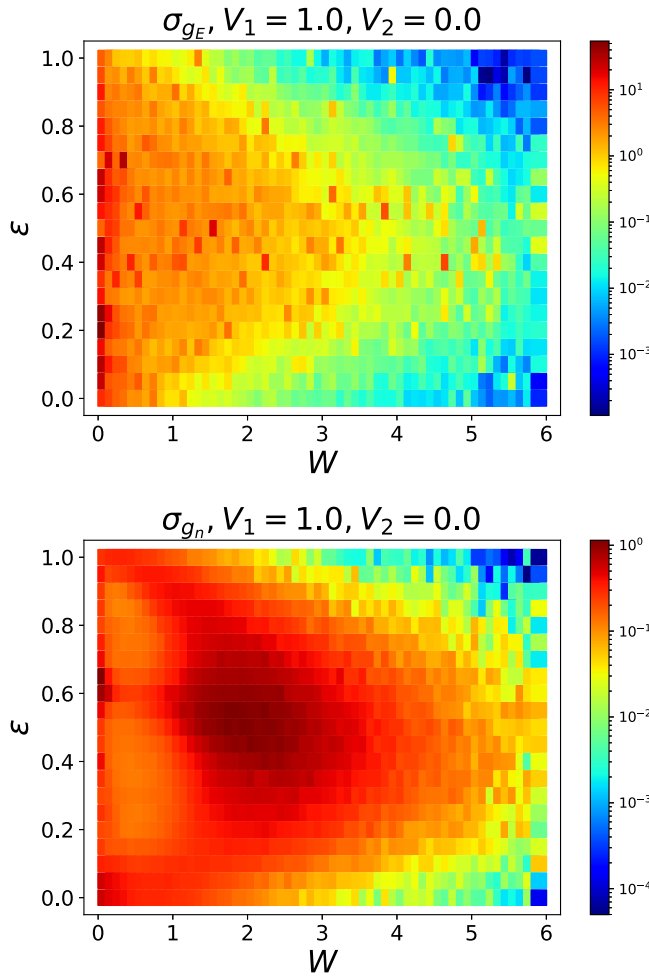


FIG. 7. Standard deviation of  $g_E$  (upper panel) and  $g_n$  (lower panel) for the entire spectrum of the energy as we change the disorder strength  $W$  for the NN interaction case ( $V_1 = 1, V_2 = 0$ ). System size  $L = 14, N = 7$ . Number of samples is 2000 for each data point.

the entanglement entropy) are calculated; it is shown that they can be used as a characterization of the localized-delocalized phase transition.

For the interacting case, we know that the single-particle density-matrix eigenstates are localized (delocalized) in the localized (delocalized) phase [52]; thus we put one step

forward and conjecture that the ETH phase can be distinguished from the MBL phase by analyzing the shifts of the occupation numbers when we change boundary conditions. In particular, we change the boundary condition from periodic to antiperiodic (as described in Sec. II) and calculate the shifts in the occupation numbers of the single-particle density matrix  $\delta n$ .

In Fig. 3 we plot occupation numbers for the NN interaction case of Eq. (2), corresponding to  $V_1 = 1, V_2 = 0$ , for periodic and antiperiodic boundary conditions in extended and MBL phases. Here just one sample is considered without disorder averaging. We can see that in the MBL phase, occupation numbers corresponding to PBC and APBC are almost identical and the shifts are negligible; in contrast, we get a nonvanishing change of the occupation numbers in the extended phase.

To have a characterization independent of the system size, we divide  $\delta n$  to average level spacing for occupation numbers  $\Delta n$  and introduce the following as an ETH-MBL phase transition characterization:

$$g_n = \delta n / \Delta n. \quad (9)$$

We plot typical averaged  $g_n$  for the NN case of Eq. (2) ( $V_1 = 1, V_2 = 0$ ) for some selected values of  $\epsilon$ , as we change disorder strength  $W$  in Fig. 4. We see that deep in the delocalized phase, shifts in the eigenvalues of the density matrix are on the order of level spacing of the eigenvalues, and it vanishes in the localized phase. At the middle of the spectrum ( $\epsilon = 0.5$ ), we obtain  $W_c \approx 3.6$ , consistent with the previously obtained results [56,58–60]. We see that  $g_n$  is not symmetric around the middle of the spectrum and is tilted toward smaller  $\epsilon$ .

By looking at  $g_n$ , we can locate mobility edges, the points in the energy spectrum, for a fixed value of disorder strength where the phase changes between delocalized and localized. We calculate  $g_n$  for a fixed value of  $W$  as we change  $\epsilon$ . The results are plotted in Fig. 5. As we can see, there are no mobility edges deep in the localized phase and deep in the delocalized phase, i.e., for  $W = 1.0$  and  $W = 4.5$ . For  $W = 1.0$ ,  $g_n$  is always nonzero, while for  $W = 4.5$  it vanishes for all values of  $\epsilon$ . For other disorder strength values, we can see mobility edges where  $g_n$  goes to zero. All this information can be summarized in Fig. 6, where  $g_n$  is calculated for the entire energy spectrum as we change disorder strength  $W$  (standard deviation of  $g_n$  is plotted in Fig. 7).

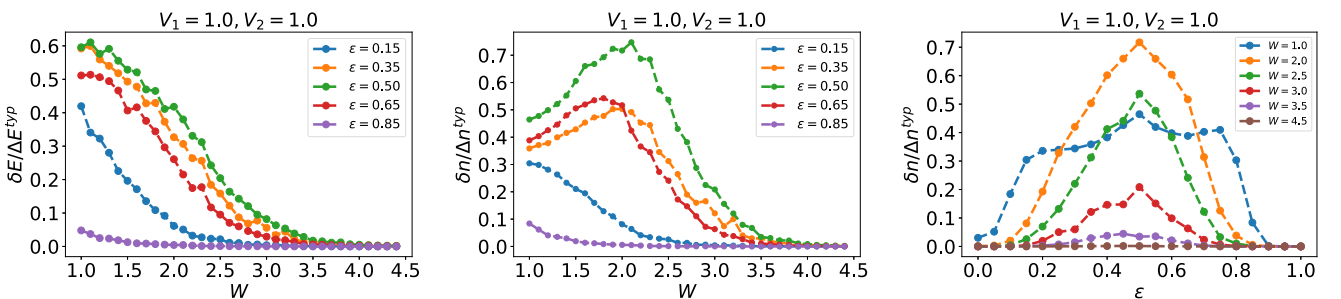


FIG. 8. Typical averaged  $g_E = \frac{\delta E}{\Delta E}$  (left panel) and  $g_n = \frac{\delta n}{\Delta n}$  (middle panel) for the case of having both NN and NNN interactions corresponding to  $V_1 = 1, V_2 = 1$  in Eq. (2) for some specific  $\epsilon$ 's as disorder strength  $W$  varies. Right panel: typical averaged  $g_n = \frac{\delta n}{\Delta n}$  for the case of NN and NNN interactions for some selected values of disorder strength  $W$  as energy varies, where we can see the mobility edges. For all plots, we set  $L = 14, N = 7$ . We take a typical average over altogether 2000 samples for each data point.

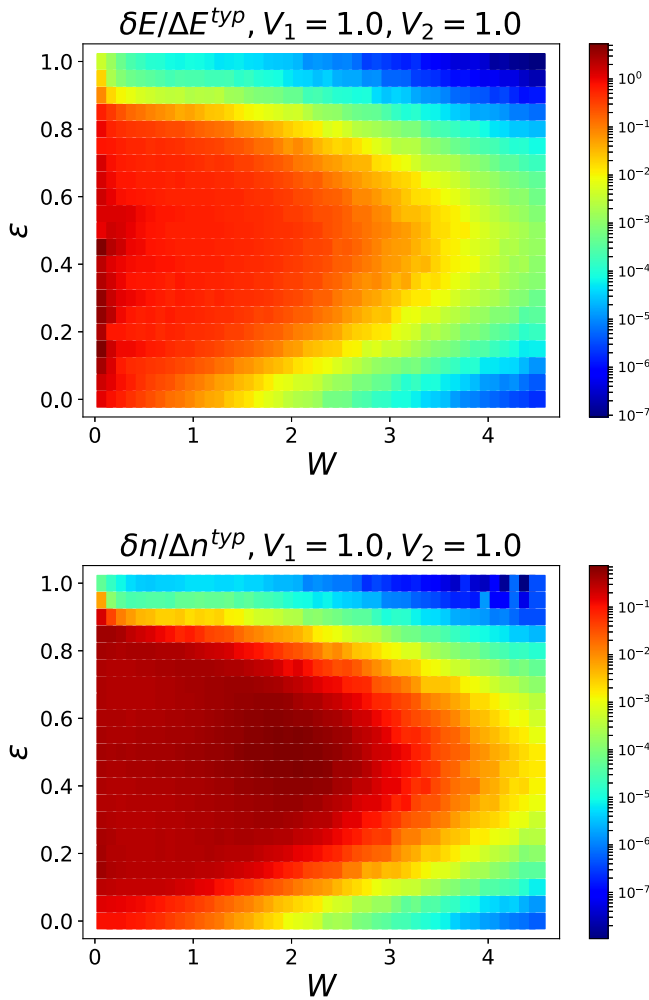


FIG. 9. Typical average of  $g_E = \frac{\delta E}{\Delta E}$  (upper panel) and  $g_n = \frac{\delta n}{\Delta n}$  (lower panel) for the entire spectrum of the energy as we change the disorder strength  $W$  for the case of having both NN and NNN interactions corresponding to  $V_1 = 1, V_2 = 1$  in Eq. (2). We set  $L = 14, N = 7$ . We take a typical average over altogether 2000 samples for each data point.

### V. NEAREST-NEIGHBOR AND NEXT-NEAREST-NEIGHBOR INTERACTIONS

It is also instructive to apply our method of characterizing the ETH-MBL phase transition to the case of having both NN and NNN interactions, corresponding to  $V_1 = 1, V_2 = 1$  in

Eq. (2). Having NNN interaction in addition to the NN interaction makes localization harder, i.e., we expect that a larger amount of disorder is required to make the state localized at each energy, and thus a transition from the ETH to MBL phase happens at a larger value of  $W_c$  compared to the NN case. The obtained results of  $g_E$  and  $g_n$  for the case of  $V_1 = 1, V_2 = 1$  are plotted in Figs. 8 and 9. As we expected, the transition point moves to larger values of disorder strength. We also see that the transition points become more asymmetric compared to the NN case. Moreover, there is no phase transition between ETH and MBL for states with the largest  $\epsilon$ 's, and those states are localized with a nonzero disorder strength.

### VI. CONCLUSION

Regarding the ETH-MBL phase transition in random interacting systems, finding the phase characterizations is a main research focus today. In this work we introduce methods for characterizing the phase transition, namely, we studied the response of the system to the boundary conditions. For free fermions, the effect of change in boundary conditions on single-particle eigenenergies [55], as well as on the single-particle density matrix [62], has been studied before. Extended eigenstates are affected by what happens at the boundary, while changes in boundary conditions are not reflected in the localized phase. We extend this idea to the interacting case. In particular, we changed the boundary conditions between periodic and antiperiodic, and then we studied the echo of these changes in the energy of the system and eigenvalues of the single-particle density matrix. We used these characterizations for the case of a 1D model with nearest-neighbor interaction, nearest-neighbor hopping, and disorder which is added by random on-site energies. This model has been studied before, and we approximately know the phase transition point. We could identify the ETH phase with significant shifts in the system's energy and significant shifts in the occupation numbers (both shifts are on the order of corresponding level spacing). In contrast, the MBL phase exhibits a vanishing response to the change in the boundary conditions. Furthermore, we added extra next-nearest-neighbor interactions and studied their effects on the ETH-MBL phase transition.

### ACKNOWLEDGMENTS

This work was supported by the Iran National Science Foundation (INSF) and the University of Mazandaran (M.P.).

- 
- [1] P. W. Anderson, *Phys. Rev.* **109**, 1492 (1958).
  - [2] R. Horodecki, P. Horodecki, M. Horodecki, and K. Horodecki, *Rev. Mod. Phys.* **81**, 865 (2009).
  - [3] F. Evers and A. D. Mirlin, *Rev. Mod. Phys.* **80**, 1355 (2008).
  - [4] A. MacKinnon and B. Kramer, *Phys. Rev. Lett.* **47**, 1546 (1981).
  - [5] E. N. Economou and M. H. Cohen, *Phys. Rev. B* **5**, 2931 (1972).
  - [6] F. M. Izrailev and A. A. Krokhnin, *Phys. Rev. Lett.* **82**, 4062 (1999).
  - [7] R. Nandkishore and D. A. Huse, *Annu. Rev. Condens. Matter Phys.* **6**, 15 (2015).
  - [8] E. Altman, *Nat. Phys.* **14**, 979 (2018).
  - [9] D. A. Abanin, E. Altman, I. Bloch, and M. Serbyn, *Rev. Mod. Phys.* **91**, 021001 (2019).
  - [10] D. Basko, I. Aleiner, and B. Altshuler, *Ann. Phys.* **321**, 1126 (2006).
  - [11] S. A. Parameswaran, A. C. Potter, and R. Vasseur, *Ann. Phys.* **529**, 1600302 (2017).
  - [12] F. Alet and N. Laflorencie, *C. R. Phys.* **19**, 498 (2018).

- [13] E. Altman and R. Vosk, *Annu. Rev. Condens. Matter Phys.* **6**, 383 (2015).
- [14] J. M. Deutsch, *Phys. Rev. A* **43**, 2046 (1991).
- [15] M. Srednicki, *Phys. Rev. E* **50**, 888 (1994).
- [16] M. Rigol, V. Dunjko, and M. Olshanii, *Nature (London)* **452**, 854 (2008).
- [17] J. M. Deutsch, *Rep. Prog. Phys.* **81**, 082001 (2018).
- [18] E. Baygan, S. P. Lim, and D. N. Sheng, *Phys. Rev. B* **92**, 195153 (2015).
- [19] X. Li, S. Ganeshan, J. H. Pixley, and S. Das Sarma, *Phys. Rev. Lett.* **115**, 186601 (2015).
- [20] I. Bloch, J. Dalibard, and W. Zwerger, *Rev. Mod. Phys.* **80**, 885 (2008).
- [21] J. Smith, A. Lee, P. Richerme, B. Neyenhuis, P. W. Hess, P. Hauke, M. Heyl, D. A. Huse, and C. Monroe, *Nat. Phys.* **12**, 907 (2016).
- [22] T. Langen, R. Geiger, and J. Schmiedmayer, *Annu. Rev. Condens. Matter Phys.* **6**, 201 (2015).
- [23] C. Chin, R. Grimm, P. Julienne, and E. Tiesinga, *Rev. Mod. Phys.* **82**, 1225 (2010).
- [24] A. M. Kaufman, M. E. Tai, A. Lukin, M. Rispoli, R. Schittko, P. M. Preiss, and M. Greiner, *Science* **353**, 794 (2016).
- [25] P. Bordia, H. Lüschen, U. Schneider, M. Knap, and I. Bloch, *Nat. Phys.* **13**, 460 (2017).
- [26] J.-y. Choi, S. Hild, J. Zeiher, P. Schauß, A. Rubio-Abadal, T. Yefsah, V. Khemani, D. A. Huse, I. Bloch, and C. Gross, *Science* **352**, 1547 (2016).
- [27] P. Bordia, H. P. Lüschen, S. S. Hodgman, M. Schreiber, I. Bloch, and U. Schneider, *Phys. Rev. Lett.* **116**, 140401 (2016).
- [28] M. Schreiber, S. S. Hodgman, P. Bordia, H. P. Lüschen, M. H. Fischer, R. Vosk, E. Altman, U. Schneider, and I. Bloch, *Science* **349**, 842 (2015).
- [29] L. Sapienza, H. Thyrestrup, S. Stobbe, P. D. Garcia, S. Smolka, and P. Lodahl, *Science* **327**, 1352 (2010).
- [30] Z. Papić, E. M. Stoudenmire, and D. A. Abanin, *Ann. Phys.* **362**, 714 (2015).
- [31] X. Li, D.-L. Deng, Y.-L. Wu, and S. Das Sarma, *Phys. Rev. B* **95**, 020201(R) (2017).
- [32] Y. Bar Lev, D. R. Reichman, and Y. Sagi, *Phys. Rev. B* **94**, 201116(R) (2016).
- [33] N. Y. Yao, C. R. Laumann, J. I. Cirac, M. D. Lukin, and J. E. Moore, *Phys. Rev. Lett.* **117**, 240601 (2016).
- [34] A. Smith, J. Knolle, D. L. Kovrizhin, and R. Moessner, *Phys. Rev. Lett.* **118**, 266601 (2017).
- [35] W. De Roeck and F. Huveneers, *Phys. Rev. B* **90**, 165137 (2014).
- [36] R. Modak and S. Mukerjee, *Phys. Rev. Lett.* **115**, 230401 (2015).
- [37] X. Li, J. H. Pixley, D.-L. Deng, S. Ganeshan, and S. Das Sarma, *Phys. Rev. B* **93**, 184204 (2016).
- [38] S. Choudhury, E.-a. Kim, and Q. Zhou, [arXiv:1807.05969](https://arxiv.org/abs/1807.05969).
- [39] M. Schulz, C. A. Hooley, R. Moessner, and F. Pollmann, *Phys. Rev. Lett.* **122**, 040606 (2019).
- [40] J. A. Kjäll, J. H. Bardarson, and F. Pollmann, *Phys. Rev. Lett.* **113**, 107204 (2014).
- [41] S. D. Geraedts, N. Regnault, and R. M. Nandkishore, *New J. Phys.* **19**, 113021 (2017).
- [42] N. Laflorencie, *Phys. Rep.* **646**, 1 (2016).
- [43] J. H. Bardarson, F. Pollmann, and J. E. Moore, *Phys. Rev. Lett.* **109**, 017202 (2012).
- [44] M. Serbyn, Z. Papić, and D. A. Abanin, *Phys. Rev. Lett.* **110**, 260601 (2013).
- [45] V. Khemani, S. P. Lim, D. N. Sheng, and D. A. Huse, *Phys. Rev. X* **7**, 021013 (2017).
- [46] B. Richard, *Ann. Phys.* **529**, 1700042 (2017).
- [47] V. Oganesyan and D. A. Huse, *Phys. Rev. B* **75**, 155111 (2007).
- [48] A. Maksymov, P. Sierant, and J. Zakrzewski, *Phys. Rev. B* **99**, 224202 (2019).
- [49] W.-J. Rao, *J. Phys.: Condens. Matter* **30**, 395902 (2018).
- [50] M. Filippone, P. W. Brouwer, J. Eisert, and F. von Oppen, *Phys. Rev. B* **94**, 201112(R) (2016).
- [51] A. De Luca, B. L. Altshuler, V. E. Kravtsov, and A. Scardicchio, *Phys. Rev. Lett.* **113**, 046806 (2014).
- [52] S. Bera, H. Schomerus, F. Heidrich-Meisner, and J. H. Bardarson, *Phys. Rev. Lett.* **115**, 046603 (2015).
- [53] S. Bera, T. Martync, H. Schomerus, F. Heidrich-Meisner, and J. H. Bardarson, *Ann. Phys.* **529**, 1600356 (2017).
- [54] S.-H. Lin, B. Sbierski, F. Dorfner, C. Karrasch, and F. Heidrich-Meisner, *SciPost Phys.* **4**, 002 (2018).
- [55] J. T. Edwards and D. J. Thouless, *J. Phys. C* **5**, 807 (1972).
- [56] M. Serbyn, Z. Papić, and D. A. Abanin, *Phys. Rev. B* **96**, 104201 (2017).
- [57] V. Khemani, R. Nandkishore, and S. L. Sondhi, *Nat. Phys.* **11**, 560 (2015).
- [58] D. J. Luitz, N. Laflorencie, and F. Alet, *Phys. Rev. B* **91**, 081103(R) (2015).
- [59] J. L. C. da C. Filho, A. Saguia, L. F. Santos, and M. S. Sarandy, *Phys. Rev. B* **96**, 014204 (2017).
- [60] B. Villalonga, X. Yu, D. J. Luitz, and B. K. Clark, *Phys. Rev. B* **97**, 104406 (2018).
- [61] I. Peschel, *J. Phys. A: Math. Gen.* **36**, L205 (2003).
- [62] M. Pouranvari and A. Montakhab, *Phys. Rev. B* **96**, 045123 (2017).